



iJRASET

International Journal For Research in
Applied Science and Engineering Technology



INTERNATIONAL JOURNAL FOR RESEARCH

IN APPLIED SCIENCE & ENGINEERING TECHNOLOGY

Volume: 5

Issue: XII

Month of publication: December 2017

DOI:

www.ijraset.com

Call: ☎ 08813907089

E-mail ID: ijraset@gmail.com

Preparation of a New Carbon/g-C₃N₄ Composite and Its Photocatalytic Activity

JebaJeeva Rani M¹, Allen Gnana Raj G²

^{1,2}Department of Chemistry and Research Centre, Scott Christian College (Autonomous), Nagercoil, K.K. Dist, Tamil Nadu, India.

Abstract: Novel activated carbon-graphitic carbon nitride (CNC) composite photocatalyst was synthesized by impregnation method. The resulting CNC composite photocatalyst was characterized by X-ray diffraction (XRD), Scanning electron microscopy (SEM) with EDAX, Fourier transform infrared spectroscopy (FT-IR). The photocatalytic activity of the novel photocatalyst was evaluated using Rhodamine B (Rh-B) as a target pollutant. The CNC composite sample exhibit enhanced photocatalytic performance under visible light irradiation than pure g-C₃N₄. The synergistic effect between carbon and g-C₃N₄ is found to be an improved photo generated carrier separation. The complete mineralization of Rh-B is determined by Chemical oxygen demand (COD) analysis.

Keywords: Activated carbon, Carbon nitride, Composite photo catalyst, Melamine, Rhoda mine B.

I. INTRODUCTION

Photocatalysis is an attractive yet challenging process to convert solar energy in to chemical energy. During the past 30 years, various inorganic semiconductors and molecular assemblies have been developed as catalysts for hydrogen production from water and as an environmental purification under visible light [1, 2]. However, the most stable metal oxide photocatalysts suffer from no or limited visible light absorption due to their large band gap [3]. For photocatalysis, precious-metal species must be used in most cases as extra co-catalysts to promote the transfer of photo induced charge carriers from bulk to the surface at which organic dyes are converted into CO₂ and H₂O. Synthetic polymer semiconductors have also been used for dye degradation; however they are active only in the ultraviolet region and have moderate performance. Here another simple polymer like semiconductor made of only carbon and nitrogen can function as a metal-free photocatalyst under visible light. Carbon nitride can exist in several allotropes with diverse properties but the graphitic phase is regarded as the most suitable under ambient conditions. The novel photocatalyst exhibits activity for the removal of organic pollutants under visible light irradiation [4], clearly demonstrating that the metal-free g-C₃N₄ photocatalyst possesses an interesting electronic properties as well as high thermal and chemical stability, therefore making them valuable materials for photocatalysis applications. However, to date the photocatalytic efficiency of bare g-C₃N₄ is still limited due to the higher recombination rate of photo generated electron-hole pairs. Many methods have been used to extend the photocatalytic performance such as doping with metals or non-metal elementals [5] and coupling with other semiconductors [6]. These methods are effective because the high surface area and small particle size it enhance e⁻-h⁺ pairs separation [7].

In this work, for the first time carbon/ g-C₃N₄ (CNC) composite was synthesized by impregnation method. The composite should increase the visible light harvesting efficiency by increasing the surface area and to evaluate the photo degradation of Rh-B under visible-light irradiation

II. EXPERIMENTAL

Melamine and activated carbon were purchased from Sigma-Aldrich. All other reagents were of analytical grade and were used as without further purification.

A. Synthesis of photocatalysts

The metal free graphitic carbon nitride (g-C₃N₄) powder was synthesized by thermal treatment of precursor melamine and it was placed in a crucible with a cover under ambient pressure in air. After dried at 80 °C for 24 h, the precursor was put in a Muffle furnace and heated to 550 °C for 3 h with a heating rate of 10 °C min⁻¹. The resultant yellow product was collected and ground into a powder for further use.

CNC composite photocatalyst was prepared as follows:

Carbon doped g-C₃N₄ composite photocatalyst was prepared by an impregnation method. Synthesis involved mixing calculated quantities of the above prepared CN powder and activated carbon in the ratio 10:1 was dispersed in 1 M HCl and deionized water.

The dispersion was magnetically stirred for 3 h. After that the product was collected by centrifugation and washed with ethanol and deionized water. Finally the sample was dried at 80 °C in an oven for 1 h. The obtained CNC was in the form of grey powder.

B. Characterization Techniques

X-ray diffraction (XRD) analysis was carried out at room temperature with a Bruker D8 advance diffract meter. The patterns were run with Cu K α radiation at a scan rate of 20-80 °C. UV-Visible spectral data were collected over a spectral range 200-800 nm with Shimadzu UV-3101 PC spectrophotometer. Fourier transform-Infra red spectra (FT-IR) in transmittance mode were recorded for a solid mixture of sample and KBr in the form of pellets on a SHIMADZU FTIR spectrometer in the frequency range 4000 to 400 cm⁻¹ with a spectral resolution of 16 (1 cm⁻¹) and an accumulation of 70 scans at room temperature. Scanning electron microscope (SEM) analysis was performed on platinum coated samples using a JOEL apparatus model JSM-5610 LV. Elemental analysis was performed by energy dispersive X-ray micro analysis (EDAX) using BRUKER-10498 model instrument.

C. Evaluation of photocatalysts

The photocatalytic degradation of Rh-B was performed under the natural sunlight in the presence of CNC composite photocatalysts. In the photocatalytic treatment of dye, a known concentration of Rh-B dye solution 1 \times 10⁻⁵M (5 mg/l) was prepared in deionized water resulting in a solution with pH 7.6 was taken in a borosil glass beaker of 250 ml capacity. 0.1 g photocatalyst was added to the 50 ml (2 g/l) of dye solution. Before irradiation of the dye solution, the suspension was stirred for 30 min in the dark to realize adsorption-desorption equilibrium in the presence of catalyst. The dye solution was agitated with an electromagnetic stirrer at a constant speed of 790 rpm. The dye solution was directly exposed to sunlight radiation in an open atmosphere. At given intervals of irradiation a known volume of sample along with the catalyst particles were collected, centrifuged and then filtered through Millipore filter paper. The filtrates were analyzed by UV-Visible spectrophotometer. The determination wavelength is 553 nm for Rh-B dye, which is the maximum absorption wavelength.

The degradation efficiency of dye is calculated by the following equation

$$\text{Degradation efficiency (\%)} = \frac{C_0 - C}{C_0} \times 100$$

Where, C₀ is the initial concentration of dye before irradiation and C is the concentration of dye after a certain irradiation time.

III. RESULTS AND DISCUSSION

A. Characterization of metal free CNC composite sample

The crystalline and phase structure of the pure g-C₃N₄ is determined by X-ray diffraction (XRD) as shown in Fig.1. The X-Ray diffraction patterns of pure graphitic carbon nitride revealed an intense broad peak at 2 θ value of 27.57°, indexed to (002) planes which is a characteristic indicator of layered stacking with a distance of 0.326 nm in the conjugated aromatic system and the inplanar repeating tri-s-triazine unit with a period of 0.675 nm can be observed from the diffraction peak at 2 θ = 13.12°, indexed with (100) plane [8]. Furthermore in CNC composite two pronounced peaks at 2 θ = 27.4° and 12.28° correspond to the characteristic diffraction peaks of pure g-C₃N₄ composite. This together with the appearance of small peaks at 2 θ = 6.15°, 10.6°, 18.38°, 22.9°, 30.9° indicates the successful deposition of activated carbon on to the graphite carbon nitride layer to form CNC composite as depicted in Fig .2.

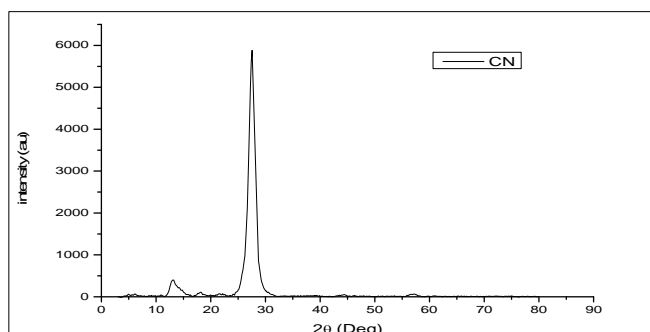


Fig.1 XRD pattern of CN composite sample.

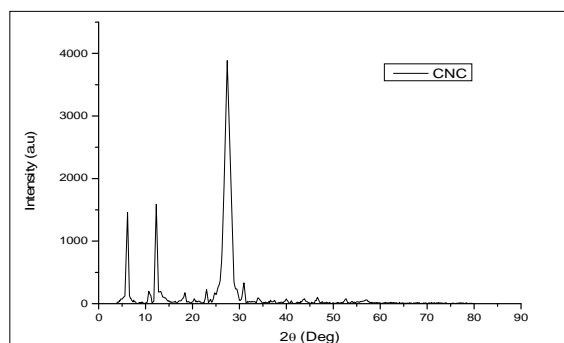


Fig.2 XRD pattern of CNC composite sample.

The molecular geometry, information about its functional groups and inter/intra molecular interactions of the resulting composite photocatalysts are characterized by FT-IR spectroscopy. Fig. 3 and Fig. 4 show the FT-IR spectra of pure g-C₃N₄ and CNC composite samples. The main characteristic peak of pure g-C₃N₄ can be assigned as follows: The main absorption bands at 1080, 1242, 1327, and 1411 cm⁻¹ is allocated to aromatic C-N stretching and the conjugated C=N stretching can be seen at 1566 and 1627 [9]. The band at 810 and 887 cm⁻¹ is attributed to out of plane bending modes of triazine units.

The FT-IR spectrum of CNC composite possesses all bands similar to that of pure g-C₃N₄. Notably after doping activated carbon, a new band emerges at 1095 cm⁻¹, which likely originates from the coupling between C-N stretching vibration of g-C₃N₄ and the C-C stretching vibration of activated carbon and also the peak at 3263 cm⁻¹ diminished due to the absorption of moisture on the surface of carbon.

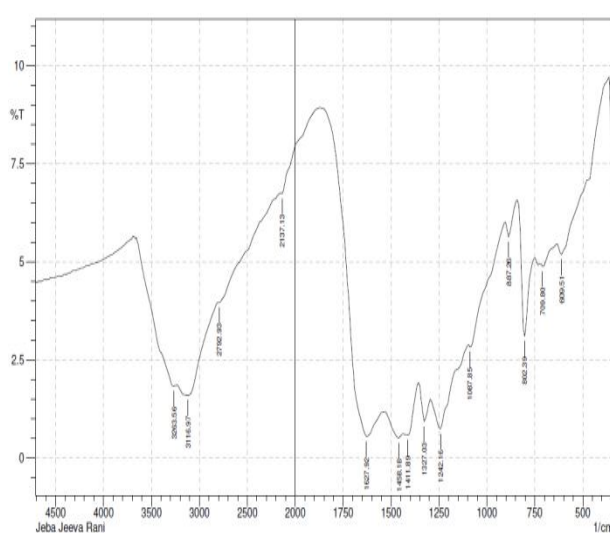


Fig. 3 FT-IR spectrum of CN

Composite sample. composite sample.

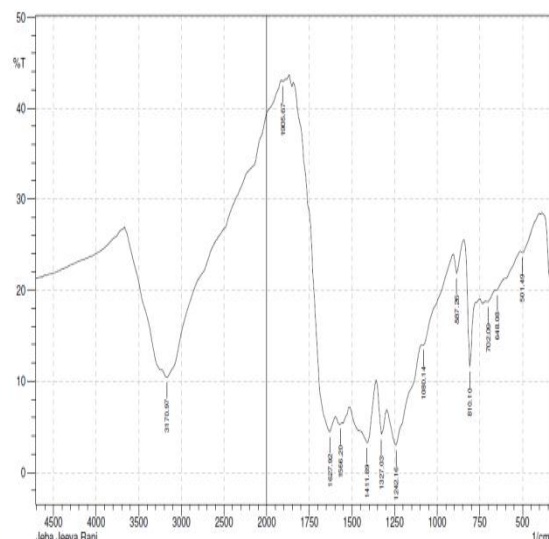


Fig. 4 FT-IR spectrum of CNC

The morphology of pure g-C₃N₄ and CNC composite samples are investigated by SEM. Fig. 5 and Fig. 6 shows the SEM images of pure g-C₃N₄ and CNC. Both the samples display aggregated morphologies. The pure g-C₃N₄ sample appears to have aggregated particles which contain many smaller crystals with the crystallite size of 16-81 nm.

After introducing activated carbon, the carbon particles deposits on the surface of g-C₃N₄ and get the tubular structure with the particle size of 10.03 nm. However, the CNC surface morphology observed in Fig.6 exhibits many acicular and small granular structures.

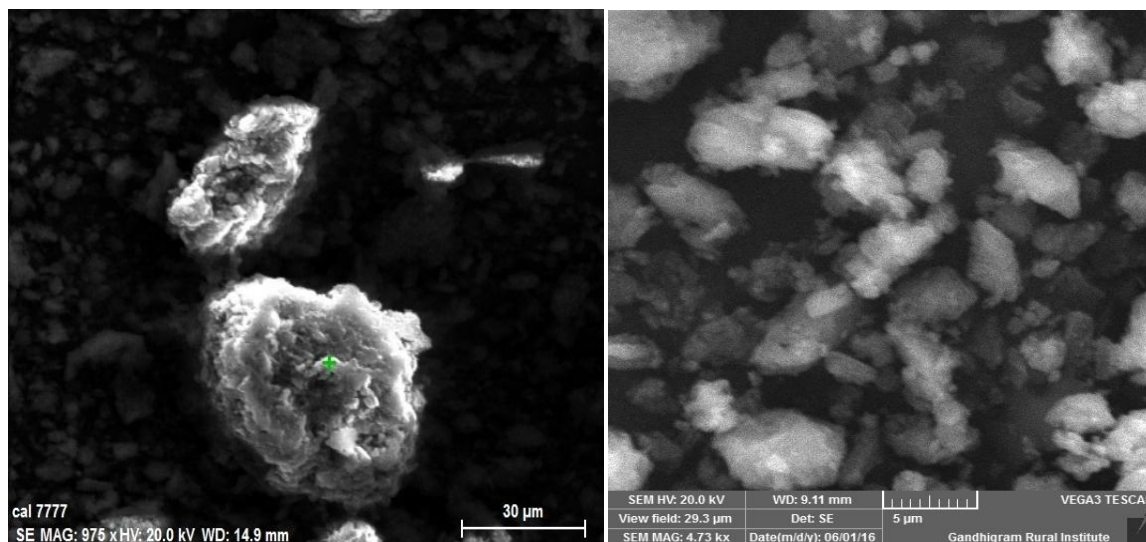


Fig. 5 SEM micrographs of CN composite sample.

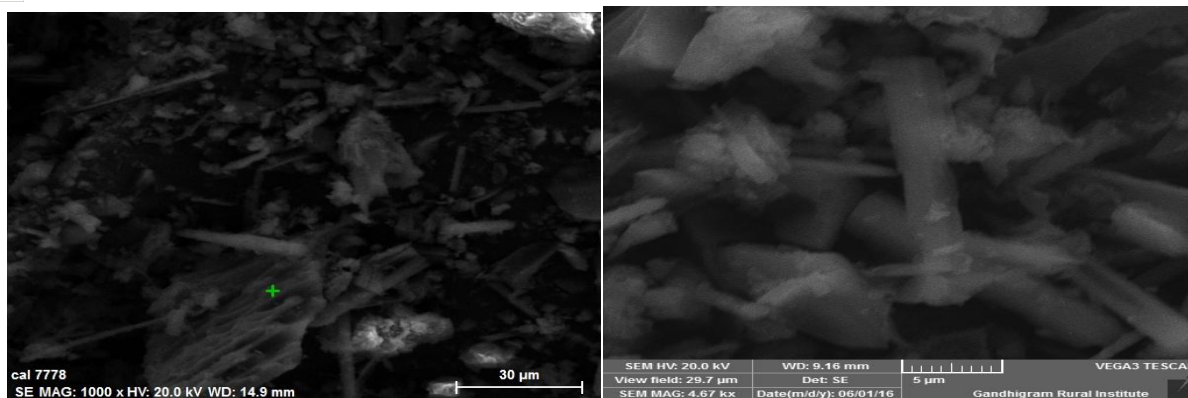


Fig. 6SEM micrographs of CNC composite sample.

The chemical stoichiometry of pure $g\text{-C}_3\text{N}_4$ and CNC composite samples are investigated with energy dispersive X-ray spectrometry analysis. It depicts as in Fig.7 and Fig.8, the results listed in Table 1 and 2. EDAX results confirmed the purity of the composite sample.

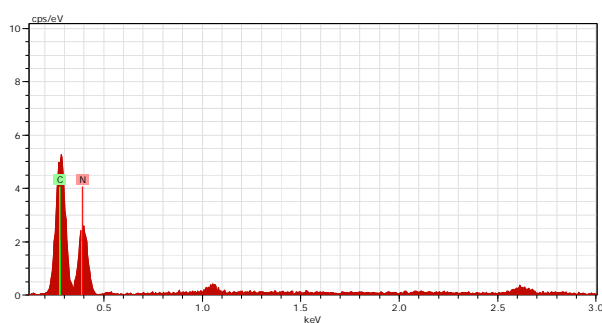


Fig. 7 EDAX spectrum of CN

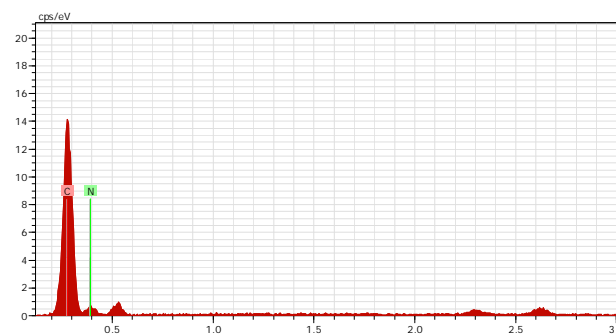


Fig. 8 EDAX spectrum of CNC

composite sample. composite sample.

Table -1Atomic and weight percentage of CN composite sample.

El AN	Series	unn. C [wt.%]	norm. C [wt.%]	Atom. C [at. %]	Error(1 Sigma) [wt.%]
N 7	K-series	58.27	58.27	56.55	17.98
C 6	K-series	41.73	41.73	43.45	8.69
	Total:	100.00	100.00	100.00	

Table -2Atomic and weight percentage of CNC composite sample.

El AN	Series	unn. C [wt.%]	norm. C [wt.%]	Atom. C [at. %]	Error(1 Sigma) [wt.%]
C 6	K-series	68.34	68.34	71.57	9.73
N 7	K-series	31.66	31.66	28.43	9.07
	Total:	100.00	100.00	100.00	

B. Photocatalytic activities

The photocatalytic activities of pure $g\text{-C}_3\text{N}_4$ and CNC composite samples are investigated by choosing the photodegradation of Rh-B dye in aqueous solution under visible light irradiation ($\lambda > 420$ nm) at room temperature. The target molecule Rh-B is relatively stable in aqueous solution upon visible light irradiation. The characteristic absorption of Rh-B at $\lambda = 553$ nm is employed to

monitor the photocatalytic degradation process. Fig. 9 (a) & (b) shows the photocatalytic activities of pure $g\text{-C}_3\text{N}_4$ and CNC composite samples under visible light irradiation.

As a comparison, Rh-B photo degradation without the photocatalyst also performed and the results demonstrated that the degradation of Rh-B is very slow in the absence of the photocatalyst under visible light irradiation. Moreover, only 40.5 % Rh-B can be photo degraded by pure $g\text{-C}_3\text{N}_4$ under visible light in 120 min. However, significantly enhanced photocatalytic performance is observed in the CNC composite sample it shows the highest activity with Rh-B degradation rate of 89 %. This enhancement of photocatalytic performance can be attributed to the synergistic effect between non-metal carbon and $g\text{-C}_3\text{N}_4$, which has an important role in the separation of electron-hole pairs.

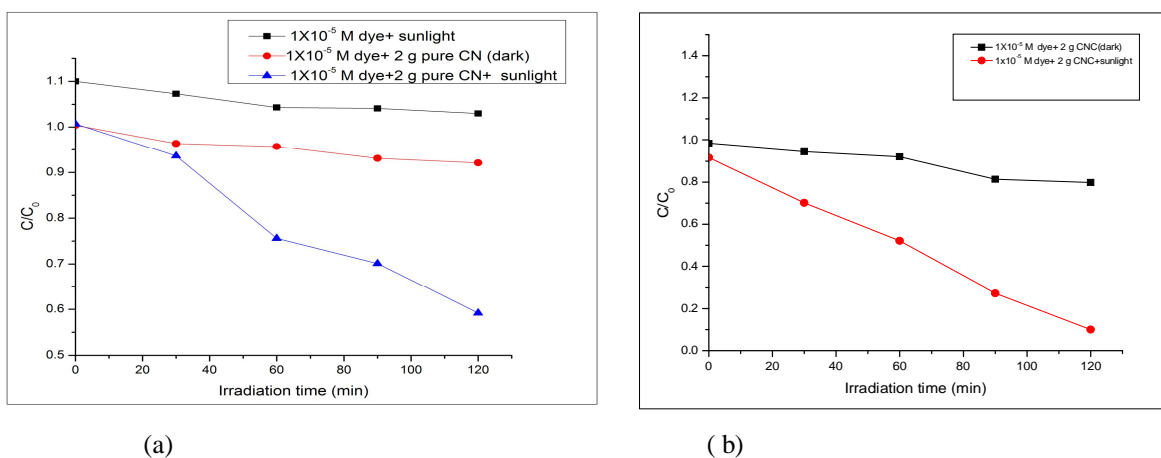


Fig. 9 Effect of incident light on the degradation of Rh-B over (a) CN (b) CNC composite samples.

The rates and efficiencies of photo assisted degradation of organic dyes are improved in the presence of oxygen. The effect of degradation of Rh-B dye in the presence of pure $g\text{-C}_3\text{N}_4$ and molecular oxygen is as shown in the Fig.10. From the graph it is observed that 45 % of dye degradation is achieved in the presence of oxygen bubbling at pH 7.6 within 120 minutes irradiation, whereas in the absence of molecular oxygen the degradation is about only 40 %. Fig.11 illustrates the degradation of Rh-B dye in the presence of CNC with and without oxygen bubbling at pH 7.6. It is observed that 94 % degradation is achieved in the presence of oxygen whereas only 89 % dye degradation is obtained without oxygen bubbling. The effect of molecular oxygen is an efficient conduction band electron trap, suppressing electron hole recombination because the conduction band of photocatalyst is nearly isoenergetic with the reduction potential of oxygen in inert solvents. So the absorbed oxygen enhances the photocatalytic activity [10].

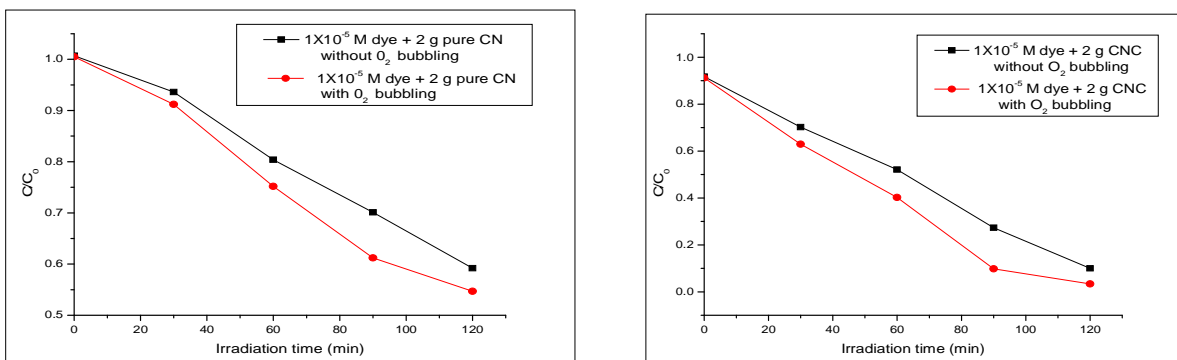


Fig. 10 and Fig. 11 Effect of O_2 bubbling on photo degradation of Rh-B over CN and CNC composite photocatalyst.

The experimental datas are fitted by applying a first order model in order to quantitatively investigate the reaction kinetics of the Rh-B degradation. Fig.12 and Fig.13 displays the pseudo first order plots for the photo degradation of Rh-B over pure $g\text{-C}_3\text{N}_4$ and CNC composite photocatalyst. The plot of the irradiation time (t) against $\ln(C_0/C)$ is nearly a straight line. The reaction constant k

can be used to evaluate the degradation rate. The CNC sample exhibits the highest photo degrading rate (k) of $0.018466 \text{ min}^{-1}$, which is about 4.1 times higher activity than that of pure $\text{g-C}_3\text{N}_4$. Therefore CNC catalyst shows excellent photocatalytic activity.

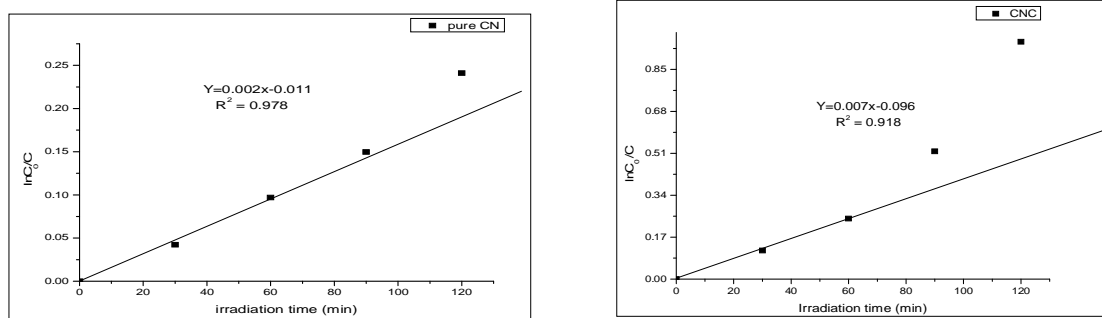


Fig. 12 and Fig. 13 First-order plots for the photo degradation of Rh-B using CN and CNC composite photocatalyst.

Each cycle, it is dried and reused for other cycles. Fig.14 illustrates the cyclic runs of Rh-B degradation using CNC photocatalysts. The Rh-B degradation rate slightly decreases after being irradiated for 360 min, which indicates sufficient stability of the CNC composite photocatalyst for Rh-B degradation.

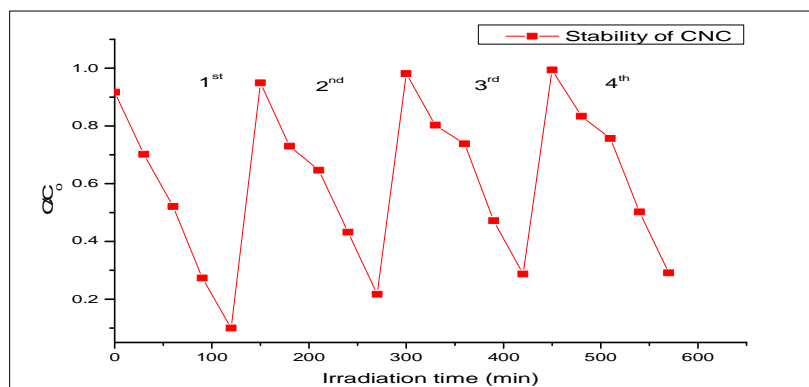


Fig. 14 Recycling runs in the photodegradation of Rh-B using CNC composite photocatalyst.

C. COD analysis

To determine the organic strength of Rh-B dye, the COD of the dye solution before and after the treatment of pure $\text{g-C}_3\text{N}_4$ and CNC composites are estimated. For pure $\text{g-C}_3\text{N}_4$ the initial COD concentration of the Rh-B solution is 29.9 mg/l and after 2 h of visible light irradiation the COD concentration decreases to 19.9 mg/l . The COD value of Rh-B using CNC composite is found to be 5.8 mg/l after 120 min irradiation. The reduction in COD value of the treated dye solution indicates the mineralization of Rh-B dye molecule.

IV. CONCLUSION

Novel carbon- $\text{g-C}_3\text{N}_4$ composite photocatalyst is successfully prepared and characterized using XRD, FT-IR, SEM, EDAX and UV-Visible spectroscopy. The absorbance band intensity of CNC composite is found to be stronger than that of pure $\text{g-C}_3\text{N}_4$. Significantly, the photocatalytic activity of CNC under visible light irradiation increases 4.1 times for photo degradation of Rh-B under visible light irradiation in comparison to pure $\text{g-C}_3\text{N}_4$. It is indicated that the efficient photo generated electron-hole transfer and separation led to the improvement of photocatalytic performance. The effectiveness and activity of the catalyst over four cycles shows that the CNC composite photocatalyst can be recycled. The COD result shows that the large conjugated chromophore structure of Rh-B is destroyed under visible light, yielding smaller organic molecules which are non-toxic to the environment.

REFERENCES

- [1] O. Khaselev and J.A Turner, (1998), A monolithic photovoltaic-photochemical device for hydrogen production via water splitting, Science, 280: 425-
- [2] H. Kato and A. Kudo, (2001), Visible light response and photocatalytic activities of TiO_2 and SrTiO_3 photocatalysts co-doped with antimony and chromium, Journal of Physical Chemistry B, 106: 5029-5034

- [3] R. Asahi, T. Morikawa, T. Ohwaki, K. Aoki and Y.Tagu,(2001), Visible light photocatalysis in nitrogen-doped titanium oxides, Science, 293: 269-271
- [4] S.C Yan, Z.S Li and Z.G Zou, (2009),Photodegradation performance of g-C₃N₄ fabricated by directly heating melamine, Langmuir, 25: 10397.
- [5] L. Ge, C.C Han, J. Liu and Y.F Li, (2012), In situ synthesis and enhanced visible light photocatalytic activities of novel PANI-g-C₃N₄ composite photocatalysts, Journal of Materials Chemistry, 22:11843
- [6] Q.J Xiang, J.G Yu and M. Jaroniec, (2011), Preparation and enhanced visible-light photocatalytic H₂-production activity of graphene/C₃N₄ composites, Journal of Physical Chemistry C, 115: 7355.
- [7] P.V Kamat,(2008), Quantum dot solar cells, semiconductor nanocrystals as light harvesters, Journal of Physical Chemistry C, 112: 18737-18753
- [8] L.Ge, (2011), Synthesis and photocatalytic performance of novel metal-free g-C₃N₄ photocatalysts, Materials Letters, 65: 2652-2654
- [9] K. Gibson, T. Glaser, E. Mike, M. Marzini, S. Tragl, M. Binnewies,H.A Mayer and H.J Meyer (2008), Preparation of carbon nitride materials by polycondensation of the single source precursor aminodichlorotriazine, Materials Chemistry and Physics, 112: 52-56
- [10] M.A Fox and C.C Chem, (1981), Mechanistic features of the semiconductor photocatalyzed olefin-to-carbonyl oxidative cleavage, Journal of The American Chemical Society, 103: 6757-6759.

TABLE I
FONT SIZES FOR PAPERS

Font Size	Appearance (in Time New Roman or Times)		
	Regular	Bold	Italic
8	table caption (in Small Caps), figure caption, reference item		reference item (partial)
9	author email address (in Courier), cell in a table	abstract body	abstract heading (also in Bold)
10	level-1 heading (in Small Caps), paragraph		level-2 heading, level-3 heading, author affiliation
11	author name		
24	title		

All title and author details must be in single-column format and must be centered.

Every word in a title must be capitalized except for short minor words such as “a”, “an”, “and”, “as”, “at”, “by”, “for”, “from”, “if”, “in”, “into”, “on”, “or”, “of”, “the”, “to”, “with”.

Author details must not show any professional title (e.g. Managing Director), any academic title (e.g. Dr.) or any membership of any professional organization (e.g. Senior Member IEEE).

To avoid confusion, the family name must be written as the last part of each author name (e.g. John A.K. Smith).

Each affiliation must include, at the very least, the name of the company and the name of the country where the author is based (e.g. Causal Productions Pty Ltd, Australia).

Email address is compulsory for the corresponding author.

A. Section Headings

No more than 3 levels of headings should be used. All headings must be in 10pt font. Every word in a heading must be capitalized except for short minor words as listed in Section III-B.

1) *Level-1 Heading*: A level-1 heading must be in Small Caps, centered and numbered using uppercase Roman numerals. For example, see heading “III. Page Style” of this document. The two level-1 headings which must not be numbered are “Acknowledgment” and “References”.

2) *Level-2 Heading*: A level-2 heading must be in Italic, left-justified and numbered using an uppercase alphabetic letter followed by a period. For example, see heading “C. Section Headings” above.

3) *Level-3 Heading*: A level-3 heading must be indented, in *Italic* and numbered with an Arabic numeral followed by a right parenthesis. The level-3 heading must end with a colon. The body of the level-3 section immediately follows the level-3 heading in the same paragraph. For example, this paragraph begins with a level-3 heading.

B. Figures and Tables

Figures and tables must be centered in the column. Large figures and tables may span across both columns. Any table or figure that takes up more than 1 column width must be positioned either at the top or at the bottom of the page.

Graphics may be full color. All colors will be retained on the CDROM. Graphics must not use stipple fill patterns because they may not be reproduced properly. Please use only *SOLID FILL* colors which contrast well both on screen and on a black-and-white hardcopy, as shown in Fig. 1.

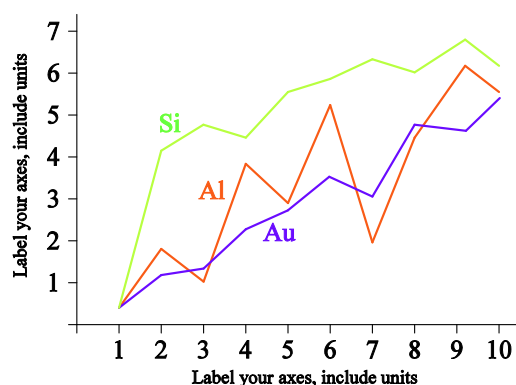


Fig.1 A sample line graph using colors which contrast well both on screen and on a black-and-white hardcopy

Fig. 2 shows an example of a low-resolution image which would not be acceptable, whereas Fig. 3 shows an example of an image with adequate resolution. Check that the resolution is adequate to reveal the important detail in the figure.

Please check all figures in your paper both on screen and on a black-and-white hardcopy. When you check your paper on a black-and-white hardcopy, please ensure that:

- the colors used in each figure contrast well,
- the image used in each figure is clear,
- all text labels in each figure are legible.

C. Figure Captions

Figures must be numbered using Arabic numerals. Figure captions must be in 8 pt Regular font. Captions of a single line (e.g. Fig. 2) must be centered whereas multi-line captions must be justified (e.g. Fig. 1). Captions with figure numbers must be placed after their associated figures, as shown in Fig. 1.



Fig.2 Example of an unacceptable low-resolution image



Fig.3Example of an image with acceptable resolution

D. Table Captions

Tables must be numbered using uppercase Roman numerals. Table captions must be centred and in 8 pt Regular font with Small Caps. Every word in a table caption must be capitalized except for short minor words as listed in Section III-B. Captions with table numbers must be placed before their associated tables, as shown in Table 1.

E. Page Numbers, Headers and Footers

Page numbers, headers and footers must not be used.

F. Links and Bookmarks

All hypertext links and section bookmarks will be removed from papers during the processing of papers for publication. If you need to refer to an Internet email address or URL in your paper, you must type out the address or URL fully in Regular font.

G. References

The heading of the References section must not be numbered. All reference items must be in 8 pt font. Please use Regular and Italic styles to distinguish different fields as shown in the References section. Number the reference items consecutively in square brackets (e.g. [1]).

When referring to a reference item, please simply use the reference number, as in [2]. Do not use “Ref. [3]” or “Reference [3]” except at the beginning of a sentence, e.g. “Reference [3] shows ...”. Multiple references are each numbered with separate brackets (e.g. [2], [3], [4]–[6]).

Examples of reference items of different categories shown in the References section include:

- example of a book in [1]
- example of a book in a series in [2]
- example of a journal article in [3]
- example of a conference paper in [4]
- example of a patent in [5]
- example of a website in [6]
- example of a web page in [7]
- example of a databook as a manual in [8]
- example of a datasheet in [9]
- example of a master’s thesis in [10]
- example of a technical report in [11]
- example of a standard in [12]

CONCLUSIONS

The version of this template is V2. Most of the formatting instructions in this document have been compiled by Causal Productions from the IEEE LaTeX style files. Causal Productions offers both A4 templates and US Letter templates for LaTeX and Microsoft Word. The LaTeX templates depend on the official IEEEtran.cls and IEEEtran.bst files, whereas the Microsoft Word templates are self-contained. Causal Productions has used its best efforts to ensure that the templates have the same appearance.

Causal Productions permits the distribution and revision of these templates on the condition that Causal Productions is credited in the revised template as follows: “original version of this template was provided by courtesy of Causal Productions (www.causalproductions.com)”.

ACKNOWLEDGMENT

The heading of the Acknowledgment section and the References section must not be numbered.

Causal Productions wishes to acknowledge Michael Shell and other contributors for developing and maintaining the IEEE LaTeX style files which have been used in the preparation of this template. To see the list of contributors, please refer to the top of file IEEETran.cls in the IEEE LaTeX distribution.

REFERENCES

- [1] S. M. Metev and V. P. Veiko, Laser Assisted Microtechnology, 2nd ed., R. M. Osgood, Jr., Ed. Berlin, Germany: Springer-Verlag, 1998.
- [2] J. Breckling, Ed., The Analysis of Directional Time Series: Applications to Wind Speed and Direction, ser. Lecture Notes in Statistics. Berlin, Germany: Springer, 1989, vol. 61.
- [3] S. Zhang, C. Zhu, J. K. O. Sin, and P. K. T. Mok, “A novel ultrathin elevated channel low-temperature poly-Si TFT,” IEEE Electron Device Lett., vol. 20, pp. 569–571, Nov. 1999.
- [4] M. Wegmuller, J. P. von der Weid, P. Oberson, and N. Gisin, “High resolution fiber distributed measurements with coherent OFDR,” in Proc. ECOC’00, 2000, paper 11.3.4, p. 109.
- [5] R. E. Sorace, V. S. Reinhardt, and S. A. Vaughn, “High-speed digital-to-RF converter,” U.S. Patent 5 668 842, Sept. 16, 1997.
- [6] (2002) The IEEE website. [Online]. Available: <http://www.ieee.org/>
- [7] M. Shell. (2002) IEEEtran homepage on CTAN. [Online]. Available: <http://www.ctan.org/tex-archive/macros/latex/contrib/supported/IEEEtran/>
- [8] FLEXChip Signal Processor (MC68175/D), Motorola, 1996.
- [9] “PDCA12-70 data sheet,” Opto Speed SA, Mezzovico, Switzerland.
- [10] A. Karnik, “Performance of TCP congestion control with rate feedback: TCP/ABR and rate adaptive TCP/IP,” M. Eng. thesis, Indian Institute of Science, Bangalore, India, Jan. 1999.
- [11] J. Padhye, V. Firoiu, and D. Towsley, “A stochastic model of TCP Reno congestion avoidance and control,” Univ. of Massachusetts, Amherst, MA, CMPSCI Tech. Rep. 99-02, 1999.
- [12] Wireless LAN Medium Access Control (MAC) and Physical Layer (PHY) Specification, IEEE Std. 802.11, 1997.



10.22214/IJRASET



45.98



IMPACT FACTOR:
7.129



IMPACT FACTOR:
7.429



INTERNATIONAL JOURNAL FOR RESEARCH

IN APPLIED SCIENCE & ENGINEERING TECHNOLOGY

Call : 08813907089  (24*7 Support on Whatsapp)